frontiers in
NEURAL CIRCUITS

ORIGINAL RESEARCH ARTICLE
published: 07 February 2012
doi: 10.3389/fncir.2012.00003

Spatiotemporal alterations of cortical network activity by selective loss of NOS-expressing interneurons

Dan Shlosberg, Yossi Buskila, Yasmin Abu-Ghanem and Yael Amitai*

Faculty of Health Sciences, Department of Physiology and Neurobiology, Ben-Gurion University of the Negev, Beer-Sheva, Israel

Edited by:
Bruno Cauli, CNRS and UPMC, France

Reviewed by:
Barry W. Connors, Brown University, USA
Kathleen S. Rockland, MIT, USA
Yoshiyuki Kubota, National Institute for Physiological Sciences, Japan

****Correspondence:***
Yael Amitai, Faculty of Health Sciences, Department of Physiology and Neurobiology, Ben-Gurion University of the Negev, POB 653, Beer-Sheva 84015, Israel.
e-mail: yaela@bgu.ac.il

Deciphering the role of GABAergic neurons in large neuronal networks such as the neocortex forms a particularly complex task as they comprise a highly diverse population. The neuronal isoform of the enzyme nitric oxide synthase (nNOS) is expressed in the neocortex by specific subsets of GABAergic neurons. These neurons can be identified in live brain slices by the nitric oxide (NO) fluorescent indicator diaminofluorescein-2 diacetate (DAF-2DA). However, this indicator was found to be highly toxic to the stained neurons. We used this feature to induce acute phototoxic damage to NO-producing neurons in cortical slices, and measured subsequent alterations in parameters of cellular and network activity. Neocortical slices were briefly incubated in DAF-2DA and then illuminated through the 4× objective. Histochemistry for NADPH-diaphorase (NADPH-d), a marker for nNOS activity, revealed elimination of staining in the illuminated areas following treatment. Whole cell recordings from several neuronal types before, during, and after illumination confirmed the selective damage to non-fast-spiking (FS) interneurons. Treated slices displayed mild disinhibition. The reversal potential of compound synaptic events on pyramidal neurons became more positive, and their decay time constant was elongated, substantiating the removal of an inhibitory conductance. The horizontal decay of local field potentials (LFPs) was significantly reduced at distances of 300–400 μm from the stimulation, but not when inhibition was non-selectively weakened with the $GABA_A$ blocker picrotoxin. Finally, whereas the depression of LFPs along short trains of 40 Hz stimuli was linearly reduced with distance or initial amplitude in control slices, this ordered relationship was disrupted in DAF-treated slices. These results reveal that NO-producing interneurons in the neocortex convey lateral inhibition to neighboring columns, and shape the spatiotemporal dynamics of the network's activity.

Keywords: epilepsy, DAF-2DA, nitric oxide, lateral inhibition, barrel cortex, dendritic delay, dendritic inhibition, synaptic integration

INTRODUCTION

It has become widely recognized that discrete inhibitory neuronal populations co-exist in the cerebral cortex and most likely contribute differentially to mold the neuronal network activity. Subtypes of interneurons possess distinct characteristics evident in typical firing patterns, peptide expression, axonal targets, or electrical coupling. These characteristics are well-correlated, implying that specific neuronal-types carry specific circuit functions (e.g., Kawaguchi and Kubota, 1993; Cauli et al., 1997; Gibson et al., 1999). For example, fast-spiking (FS), parvalbumin-expressing (PV+), proximally targeting inhibitory neurons mediate feed-forward inhibition both in the hippocampus and somatosensory cortex (Kiss et al., 1996; Beierlein and Connors, 2002), tightly control spike timing (Pouille and Scanziani, 2002), and promote gamma-band cortical oscillations (Sohal et al., 2009). On the other hand, activation of distally targeting, somatostatin-expressing (SOM+) interneurons elicits IPSPs of smaller amplitude and slower kinetics than proximally evoked IPSPs (e.g., Salin and Prince, 1996; Silberberg and Markram, 2007), and it has been proposed that these IPSPs modulate excitatory synaptic inputs locally. These neurons are recruited by high activity rates to mediate intracortical recurrent inhibition (Kapfer et al., 2007) or feed-forward thalamocortical inhibition at high activity rates (Tan et al., 2008). While intense research has been conducted to describe the cellular attributes of these interneurons subtypes, their specific roles in the network have remained largely ambiguous due to the difficulty to identify and selectively manipulate them. Optogenetics tools have already begun to reveal distinct effects of local inhibitory populations, but these techniques are not free of limitations (for review see Cardin, 2011).

The neuronal isoform of the enzyme nitric oxide synthase (nNOS) is expressed in the neocortex by specific subsets of GABAergic neurons (Karagiannis et al., 2009; Kubota et al., 2011). To simplify available data, one subset comprised mostly SOM+, dendritic targeting interneurons (Lüth et al., 1995; Gonchar and Burkhalter, 1997; Vruwink et al., 2001). Their firing properties have been commonly termed "LTS" after their tendency to fire low threshold spikes (Kawaguchi, 1993), and are identified also by deep and complex AHPs (Beierlein et al., 2003). Another group is composed of some of the neuropeptide Y-expressing (NPY+) or PV+ cells with an adapting firing pattern, which amongst

themselves also display high heterogeneity both in morphology as well as physiology (Karagiannis et al., 2009; Kubota et al., 2011). While it seems that these neuronal groups display overlap in several features, two distinct morphological features appear among the nNOS+ neurons: Neurogliaform neurons which display a dense local axonal arborization (e.g., Uematsu et al., 2008; Karagiannis et al., 2009), and in contrast—long-range projecting GABAergic interneurons, (e.g., Lüth et al., 1995; Gonchar and Burkhalter, 1997; Vruwink et al., 2001). Additional classification scheme divided nNOS-expressing (NOS+) interneurons to type I, characterized by large somata and strong nNOS or NADPH-diaphorase (NADPH-d) reactivity, and type II, characterized by small somata and weaker nNOS/NADPH-d staining (Lee and Jeon, 2005; Kubota et al., 2011).

In a previous study (Buskila et al., 2005) we identified NO-producing neurons in acute cortical slices by using the fluorescent NO indicator diaminofluorescein-2 diacetate (DAF-2DA, Kojima et al., 1998). We found that this indicator indeed stains non-pyramidal neurons in cortical slices with bright puncta which delineate some somata, but are also sparsely scattered in the neuropil. (Buskila et al., 2005, **Figure 1A**). Interestingly, these DAF-positive neurons appeared shrunken under IR/DIC optics and attempts to patch them were not successful, while other non-fluorescent neurons in the visual field were easily patched and displayed normal physiology. Moreover, propidium iodide, an indicator for cell death, was co-localized with the vast majority of DAF-positive neurons (Buskila et al., 2005). We, therefore, used DAF-2DA to induce selective phototoxic damage to NO-producing interneurons in cortical slices, and explored the cellular and network effects of this manipulation. We find that selective damage to this population results in mild disinhibition of the entire cortical network which is especially pronounced at horizontal distances of 300–400 μm from the center of activation, and in severe alterations of the spatio-temporal activity dynamics during repetitive stimulation.

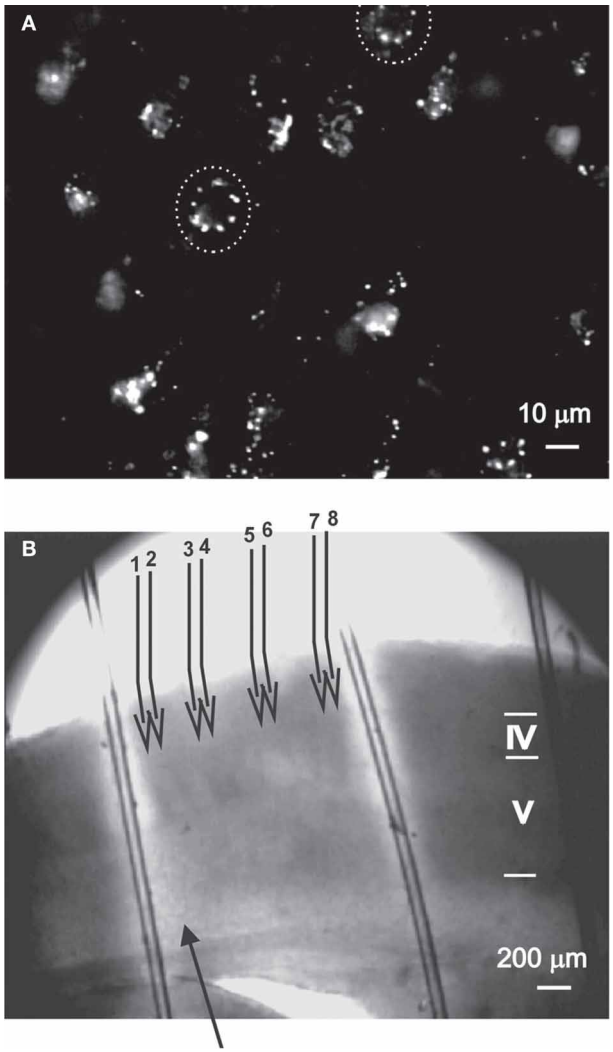

FIGURE 1 | The experimental methods used to evaluate the role of nNOS+ neurons. (A) DAF-2DA staining of neurons in acute slices, as visualized under the 40× objective (details in Buskila et al., 2005). Suspected neuronal somata are surrounded by dashed circle. **(B)** The illustration depicts the experimental paradigm. An acute slice which had been incubated in DAF-2DA is illuminated through the 4× objective (Methods, area displayed in bright light). The stimulating electrode (filled arrow) is placed above the white matter. For LFP recordings, four pairs of micropipettes (numbered open arrows) are placed in layer 2/3, where electrode #1 is in column with the stimulating electrode. Cortical lamina is marked by roman numerals.

MATERIALS AND METHODS

SLICE PREPARATION AND PHOTOTOXICITY INDUCTION

All experiments were carried out in compliance with the ethical guidelines of the NIH Guide for the Care and Use of Laboratory Animals to minimize the number of animals used and their suffering. The Animal Care Committee of Ben-Gurion University approved all procedures. Experiments were carried on mice (CD1, 14–21 days old). The mice were deeply anesthetized with pentobarbital, decapitated, and their brains quickly removed into cold (4°C) physiological solution. Thalamocortical brain slices (350 μm thick) were cut with a vibratome (Campden Instruments, London, UK) and kept in a holding chamber at room temperature for at least 1 h before any manipulation, continuously bubbled by 95% O_2–5% CO_2. The bathing solution in all experiments contained (in mM): 124 NaCl, 3 KCl, 2 $MgSO_4$, 1.25 $NaHPO_4$, 2 $CaCl_2$, 26 $NaHCO_3$, and 10 dextrose, and was saturated with 95% O_2–5% CO_2 (pH 7.4). The temperature was kept at 34°C and slices were continuously perfused. For phototoxicity induction, slices were incubated in diaminofluorescein-2 diacetate (DAF-2DA, 2 μm, Calbiochem, La Jolla, CA) for 10 min before they were transferred to the recording chamber, mounted on an upright microscope equipped with infrared/differential interference contrast (IR/DIC) optics (Nikon Physiostation EC-600, Tokyo, Japan). Illumination was performed using a light source (100 W mercury lamp) via a Nikon filter (excitation wavelength 450–490 nm, emission wavelength 520 nm), using either a 60× fluid immersion objective (for cellular recordings) or 4× objective (for area phototoxicity). Imaging was done using a black and white CCD camera with integrating frame grabber control unit (CCD-300IFG, Dage-MTI, USA), integrating 16 frames for each image. Several DAF-2DA-positive neurons could be identified in almost each visual field by punctate fluorescent

staining (**Figure 1A**, Buskila et al., 2005). Area phototoxicity was induced by exposing the slices to light in the above wave length for a period of 5 min. The light-exposed field had a diameter of about 5 mm (**Figure 1B**), thus we estimate that most of the barrel cortex in the slice was affected.

ELECTROPHYSIOLOGY

Whole-cell recordings were performed in layer 5 of the somatosensory cortex using patch pipettes (3–5 MΩ), containing (in mM): 125 *K*-gluconate, 2 $MgCl_2$, 10 Hepes, 10 EGTA, 5 NaCl, and $2Na_2ATP$. Extracellular stimulations (200 μs, 10–200 μA) were delivered through an AMPI isolation unit (Jerusalem, Israel) using a bipolar concentric microelectrode (Micro Probe Inc.) placed ∼300 μm lateral to the recording electrode to stimulate intracortical axons.

For extracellular recordings, the slices were transferred to a chamber that held the slices at the fluid-gas interface. In some experiments the $GABA_A$ receptor blocker picrotoxin (PTX, 3–8 μM, Sigma-Aldrich) was included in the perfusing solution. Local field potentials (LFPs) were recorded in layer 2/3 of the somatosensory cortex using four pairs of sharpened tungsten electrodes (Micro Probe Inc., 1–2 MΩ). The electrodes in each pair were spaced 100 μm apart and the distance between pairs was 200 μm. Stimulation was delivered vertically under the first electrode of the array and right above the white matter (**Figure 1B**).

NADPH-DIAPHORASE HISTOCHEMISTRY

At the end of recording session, slices were fixed overnight in a solution of paraformaldehyde at 4% in 0.1 M phosphate buffer (pH 7.4), then transferred to a solution of 30% sucrose for cryoprotection, and re-sectioned to 100 μm. NADPH-d histochemistry was conducted according to standard procedures. Briefly, free-floating sections were incubated in a solution containing 1 mM reduced β-NADPH (Sigma-Aldrich, Israel), 0.2 mM nitro blue tetrazolium (Sigma-Aldrich, Israel), 0.1 M phosphate buffer, 0.1% Tween (Sigma-Aldrich, Israel) at 37°C for 3–4 h. The reaction was visually controlled and stopped by washing the sections with phosphate buffered saline at pH 7.4. The sections were then mounted on slides, air-dried, and cover-slipped. Under light microscopy, NADPH-d-positive neurons and blood vessels were identifiable by the presence of dark blue staining.

STATISTICAL ANALYSIS

Statistical analysis was performed using SPSS software. We either used the analysis of variance (ANOVA) test for multiple comparisons, or the Wilcoxon test for paired data, unless noted otherwise. Results are reported as mean ± S.E.M.

RESULTS

NO-PRODUCING INTERNEURONS ARE SELECTIVELY DAMAGED

Our previous findings implied that neurons which exhibited DAF staining, hence NOS positive, were damaged by the light (Buskila et al., 2005). These neurons were expected to be a subset of inhibitory neurons, with non-FS firing properties. We wanted to make use of this finding to selectively eliminate this group, but initially we ascertained the specificity of the phototoxicity.

NADPH-d histochemistry provides a specific histochemical marker for neurons producing nitric oxide (NO) (Hope et al., 1991; Vincent and Kimura, 1992), thus we examined the effect of treatment with DAF-2DA (2 μM, 10 min incubation) and area illumination (5 min through the 4× objective) on the histochemical reaction. Untreated slices displayed a typical image of multiple darkly stained neurons scattered in the neocortex (**Figure 2A**). Higher magnification revealed a dense network of stained axons, passing in all directions (**Figure 2A**, inset). In contrast, no stained neurons were found in the neocortex in slices which had been incubated in DAF-2DA and illuminated, while such neurons appeared in the striatum and midbrain structures of the same slices, distant from the illuminated zone. Interestingly, blood vessels were clearly noted in the neocortex of those same slices following long incubation periods, but not neurons (**Figure 2B**, arrows), suggesting that the weak NADPH-d reactivity of NOS-expressing endothelial cells (e.g., Felaco et al., 2001) was less disturbed by the process. Taken together, the findings confirmed the damage to NOS-expressing neurons in the illuminated zone.

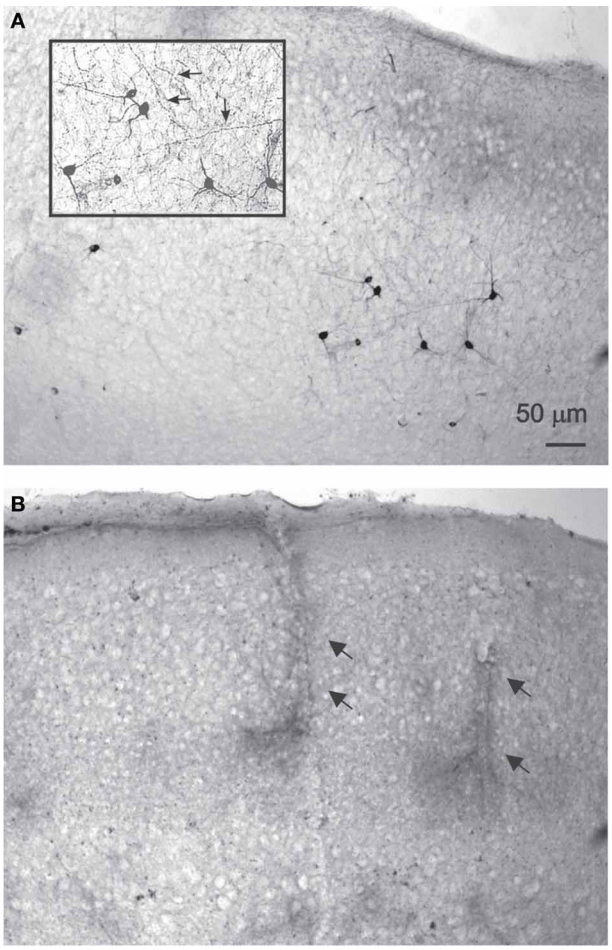

FIGURE 2 | NADPH-d staining is reduced following DAF-2DA incubation and illumination. (A) Control, untreated sections display multiple darkly stained neurons. In the inset, additional magnification highlighting the network of stained axons (arrows). **(B)** Neocortical section which had been treated by DAF-2DA and illumination. The histochemical reaction has been extended for several hours. No neurons are seen, but note darkly stained capillaries.

To further ascertain the selectivity of the damage, we also examined directly the electrophysiological response of DAF-incubated neurons to illumination. Since fluorescent neurons could not be accessed (see above), we patched neurons in layer 5 of the somatosensory cortex in slices which had been incubated in DAF-2DA before opening the fluorescent light shutter. The passive membrane properties were monitored by analyzing voltage deflections to short hyperpolarizing current pulses delivered at 1–3 Hz, before, during, and following illumination. Pyramidal neurons were initially differentiated from interneurons by the shape of their somata and proximal dendrites under IR/DIC optics. Recorded pyramidal neurons ($n = 30$) displayed either regular-spiking (RS) or intrinsically bursting firing patterns (Chagnac-Amitai et al., 1990). Their passive membrane properties remained unchanged throughout the illumination period and afterwards, as long as they were recorded (**Table 1 and Figure 3A**). Similarly, inhibitory FS interneurons, identified by their typical firing pattern (Golomb et al., 2007, $n = 6$) were not affected by the illumination process (**Figure 3B and Table 1**). Notably, none of the pyramidal or FS neurons exhibited a fluorescent response. We also recorded eight neurons which displayed elongated somata and were oriented in the vertical axis as observed under IR/DIC optics. These neurons exhibited a firing pattern which was not FS, but rather compatible with adapting or non-adapting LTS patterns (Gibson et al., 1999; Beierlein et al., 2003; Ma et al., 2006). Out of these, four neurons displayed fluorescence upon illumination (**Figure 3D**). These fluorescent neurons rapidly depolarized, fired few spikes and the recording was abruptly lost, typically within the duration of illumination (**Figure 3C**, right panel). The additional neurons did not fluoresce and a stable recording was held well after the illumination period while their membrane properties remained unchanged (data not shown). Taken together, these results verify our previous data which implied that DAF-2DA fluorescence is toxic to NO-producing neurons.

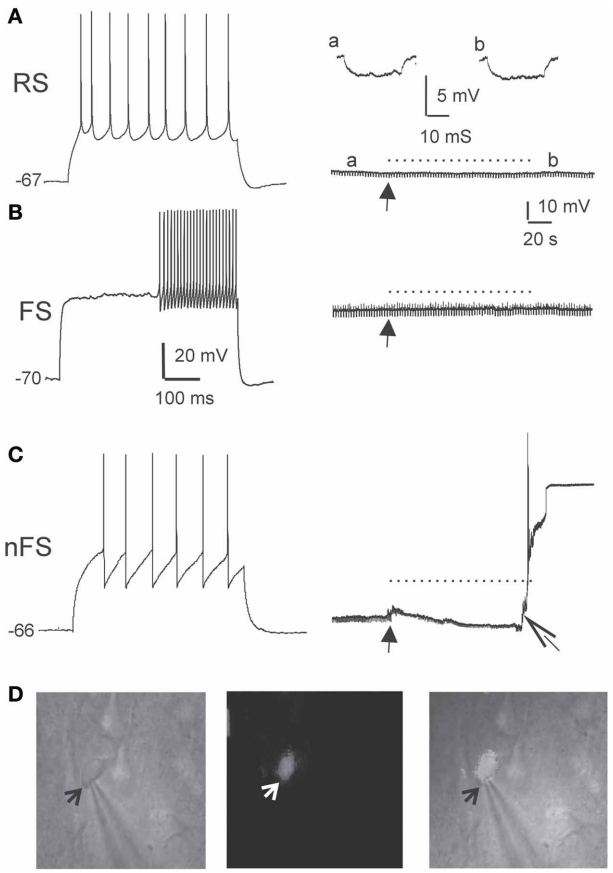

FIGURE 3 | DAF phototoxicity is selective to interneurons with LTS firing pattern. Layer 5 neurons were recorded in slices pre-incubated in DAF-2DA (2 μM, 10 min). **(A)** The left panel displays typical firing pattern of a pyramidal RS neuron in response to depolarizing current pulse. The resting potential is marked to the left. On the right—the recorded trace before opening the fluorescent shutter (arrow), during illumination (dotted line) and afterwards. A hyperpolarizing current pulse monitored the membrane resistance, and examples from time points "a" and "b" are displayed above. **(B)** Example traces of the response of a FS-type interneuron to light. Details as in **(A)**. **(C)** Example traces of the response of a LTS-type interneuron to light. Note on the right panel the appearance of instability of the membrane potential and a reduction of membrane resistance shortly after opening the shutter (closed arrow), and loss of the membrane potential shortly before the end of illumination (open arrow). **(D)** Images of the neuron in **(C)**. On the left is an IR/DIC image of the patched neuron. An arrow points to the tip of the recording pipette. The middle image shows the same field under fluorescent light, showing faint staining in the recorded neuron. On the right is a combined image.

INCREASED NETWORK EXCITABILITY FOLLOWING SELECTIVE LOSS OF NOS+ INTERNEURONS

To damage NO-producing interneurons selectively in a large cortical area, we exposed DAF-incubated slices to light for 5 min through the 4× objective, and investigated the effect of this manipulation on properties of the population activity. Initially, we tested whether the balance between excitation and inhibition in the network has been altered. As expected, the stimulus—response curve of LFPs in DAF-treated slices was steeper compared with untreated slices (**Figure 4A**, slope values – control: 0.17 ± 0.02, $n = 9$; treated: 0.27 ± 0.04, $n = 9$; $p = 0.02$ student

Table 1 | Membrane properties of pyramidal neurons and FS interneurons in DAF-treated slices were not altered by the fluorescent light.

	V_m (mV)	R_{in} (MΩ)	τ (ms)	V_m (mV)	R_{in} (MΩ)	τ (ms)
	Before illumination			After illumination		
Pyramidal ($n = 30$)	-68.4 ± 0.8	218.6 ± 19.6	20.6 ± 1.9	-68.0 ± 0.9	205.1 ± 17.6	19.1 ± 1.6
FS ($n = 6$)	-67.2 ± 1.6	99.2 ± 13.5	13.16 ± 4.6	-64.9 ± 2.6	107.1 ± 17.1	13.14 ± 3.7

Measurements were taken before opening the fluorescent light shutter and 2 min after the termination of a 5 min illumination period. V_m, resting membrane potential; R_{in}, input resistance; τ, the membrane time-constant. Note the stability of parameters throughout the manipulation.

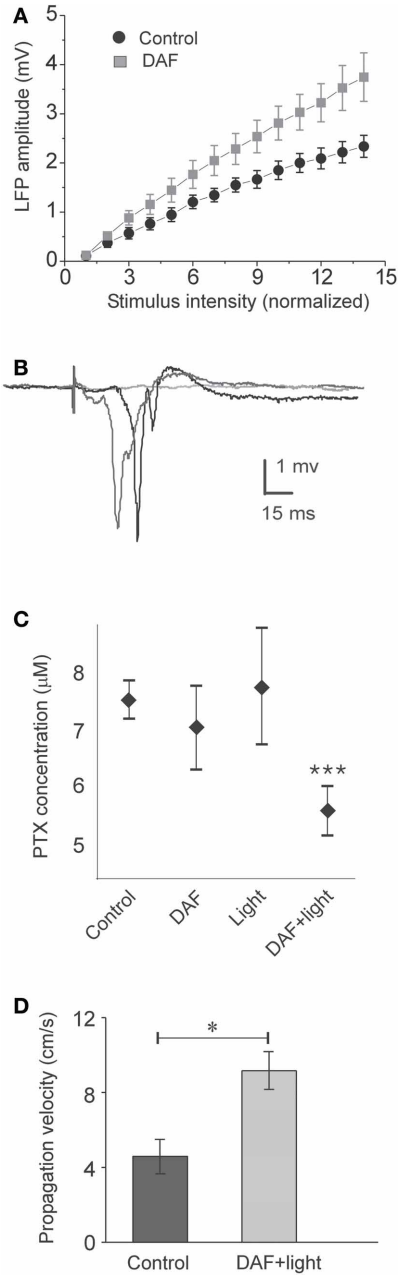

FIGURE 4 | DAF-treated slices are disinhibited. The treatment consisted of 10 min incubation in a solution containing 2 μM DAF-2DA, and 5 min fluorescent illumination through the 4× objective. **(A)** A plot of the average LFP amplitude against the normalized stimulus intensity demonstrates steeper slope for DAF-treated slice ($n = 9$) compared with control slices ($n = 9$). **(B)** An example of three consecutive traces of synchronized epileptic activity recorded at a single point in DAF-treated slice, when inhibition was further reduced by PTX (5 μM), demonstrating a failure and two synchronized events of variable latency (shades of gray). **(C)** Threshold concentrations of PTX required for eliciting epileptic activity as in **(B)**, under different conditions (control – $n = 9$; DAF-2DA – $n = 9$; light – $n = 10$; DAF-2DA + light – $n = 11$). Note significantly reduced dose in slices which have been treated with DAF and illumination. **(D)** The propagation velocity of epileptic discharge at suprathreshold concentrations of PTX is higher in DAF-pretreated slices ($n = 12$) compared with non-treated slices ($n = 13$), reflecting pre-existing disinhibition.

t-test), indicating increased network excitability. When inhibition efficacy in cortical slices is sufficiently reduced, it is possible to evoke synchronized "epileptic" population events, which appear in an all-or-none manner to threshold stimulus intensity, their latency from the stimulation is highly variable, and they can propagate horizontally along the slices without decrement (**Figure 4B**, Chagnac-Amitai and Connors, 1989; Shlosberg et al., 2003). Such synchronized population events did not appear spontaneously and could not be evoked in DAF-treated slices. We thus applied gradually increasing concentrations of the $GABA_A$ receptor blocker picrotoxin (PTX) to the perfusing solution (adding 1 μM every 30 min), noting the minimal concentration required to elicit such synchronized events as an indication of the degree of disruption in the balance between excitation and inhibition. Indeed, DAF-treated slices ($n = 11$) required significantly lower doses of PTX to achieve the pharmacological threshold to epileptic events as compared with untreated slices ($n = 9$), slices that were treated with DAF-2DA alone ($n = 9$), or slices treated with light alone ($n = 10$) ($p < 0.0001$, ANOVA, **Figure 4C**), thus confirming that the manipulation (incubation in DAF-2DA followed by illumination) reduced the inhibition in the network.

Finally, it has been shown both theoretically and experimentally that the propagation velocity of epileptic discharges is dictated by the relative strength of cortical inhibition present (Golomb and Ermentrout, 2001; Shlosberg et al., 2003; Trevelyan et al., 2007). Once epileptic events were elicited in the slices by applying a suprathreshold dose of PTX (7–8 μM), we measured their propagation velocity across a horizontal distance of 1 mm. DAF-treated slices displayed significantly higher propagation velocity than untreated slices (treated -9.2 ± 1 cm/s, $n = 12$; control -4.6 ± 0.9 cm/s, $n = 13$, $p < 0.02$, **Figure 4D**). Taken together, these results ascertain that the procedure of DAF-2DA incubation followed by illumination, shown above to damage NO-producing interneurons, resulted in a significant increase of network excitability, but not sufficiently to instigate synchronized activity.

MODULATION OF SYNAPTIC POTENTIALS FOLLOWING LOSS OF NOS+ NEURONS

A notable subset of the cortical NO-producing interneurons are dendritic–targeting (e.g., Valtschanoff et al., 1993; Lüth et al., 1995; Seress et al., 2005), hence their influence is expected to be electrotonically distant from the somatic integration zone. We explored the effect of the assumed removal of dendritic inhibition on the properties of compound synaptic potentials evoked on pyramidal neurons by activating intracortical pathways and recording PSPs before and after area illumination as above. As already noted, the membrane properties of pyramidal neurons were not altered by the illumination. The reversal potential of the synaptic events (E_{rev}) shifted to more positive values in four neurons, and did not change in two others. Overall, there was a significant adjustment in the average reversal potential of these events ($E_{rev\ control}$ -28.6 ± 7.4 mV; $E_{rev\ treated}$ -14.2 ± 9.2 mV, $p = 0.02$, $n = 6$, **Figure 5A**), indicating that some inhibition has been removed. In accordance, the change in E_{rev} was accompanied by a reduction in the conductance slope of these synaptic

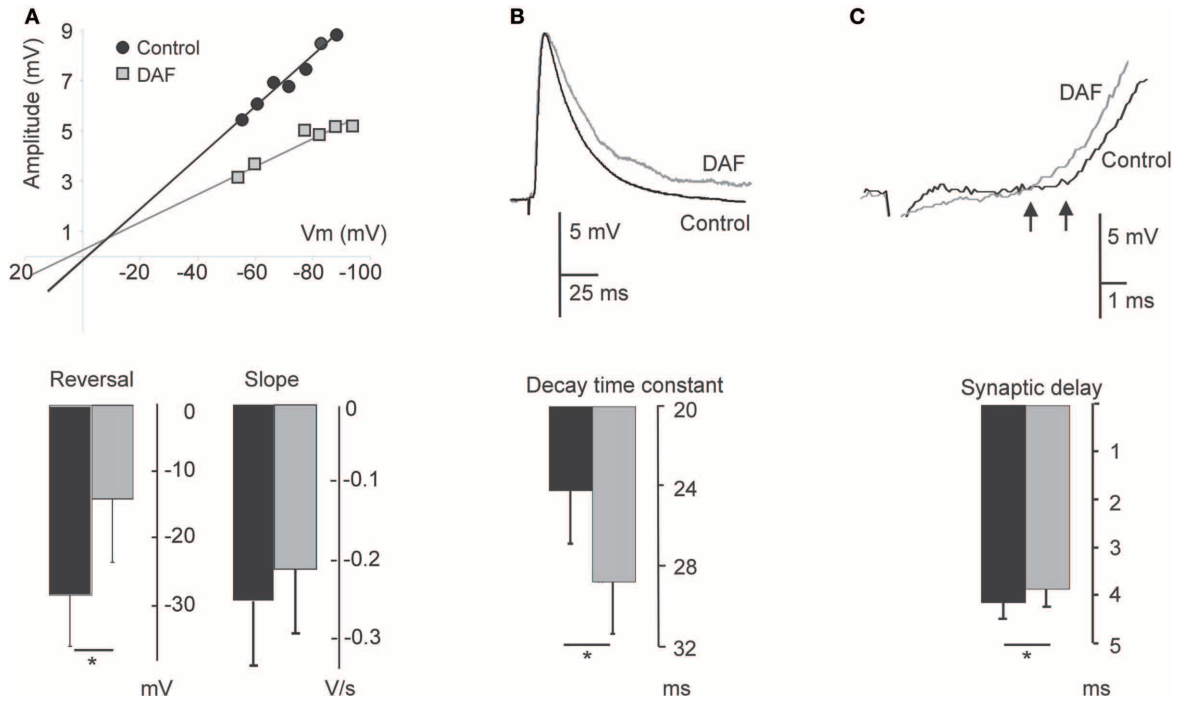

FIGURE 5 | Damage to NOS+ interneurons affects synaptic integration in pyramidal neurons. PSPs evoked on layer 5 pyramidal neurons before 2 min illumination and afterwards are compared. **(A)** Plot of the relationship between PSP amplitude and the membrane potential in a single neuron displays a change both in the reversal potential and slope conductance following illumination (upper panel). The bottom panel displays a summary diagram of these parameters for the population ($n = 6$). **(B)** Example traces of EPSPs before and after illumination, demonstrating an elongation of the decay time (upper panel). The bottom panel displays the summary diagram of the change in the decay time constant ($n = 8$). **(C)** Example traces of EPSPs before and after illumination, demonstrating a decrease in the delay. Arrows point to the deflection points (upper panel). The bottom panel displays a summary diagram of the change in the dendritic delay ($n = 8$). For all panels, recording under control conditions are represented by black bars; recordings following illumination are represented by gray bars.

events (**Figure 5A**). Assessing the shape parameter of synaptic potentials, there was no significant change in the rising slope, but we found elongation of about 17% in the PSPs decay time-constant (τ_s) ($\tau_{s\ control}$ 24.1 ± 2.7 ms; $\tau_{s\ treated}$ 28.7 ± 2.8 ms, $p = 0.018$, $n = 8$, **Figure 5B**). This finding is compatible with an increased resistance at the background of these synaptic events. Since the membrane input resistance was not altered by the illumination, we concluded that other conductances, evoked during the synaptic events, have been subtracted. In addition, a small but significant decrease in the synaptic delay appeared after the illumination (4.1 ± 0.33 ms before and 3.8 ± 0.35 ms after, $p = 0.012$, $n = 8$, **Figure 5C**), likely to reflect a reduction in the time required for the synaptic current to travel along the apical dendrites (Agmon-Snir and Segev, 1993). Altogether, the results reveal multipart modulation of excitatory synaptic integration by the removal of the inhibition mediated by NOS+ neurons.

LOSS OF NOS+ INTERNEURONS PRODUCES SPATIOTEMPORAL ALTERATIONS OF NETWORK ACTIVITY

In the neocortex, the horizontal spread of activity from a center of activation to neighboring regions is powerfully constrained by inhibition (Chagnac-Amitai and Connors, 1989). At least some NOS+ interneurons possess especially long intra-cortical or even projecting axonal arbors (Wang et al., 2004; Higo et al., 2007; Tamamaki and Tomioka, 2010), thus we conjectured that they convey lateral, inter-columnar inhibition. To test this possibility, we placed multiple extracellular microelectrodes in supragranular laminae to monitor the spread of activity by recordings LFPs at horizontal distances up to 1000 μm. When stimulating above the white matter, a typical sharp and negative LFP was recorded by the electrode positioned vertically in line (position 0, **Figure 6A**). The amplitude of LFPs decreased horizontally, reaching around 10% of its maximal amplitude at 1000 μm. The latency difference between LFPs at position 0 and at 1000 μm laterally was around 3 ms (**Figure 6B**). Such a time delay is likely to be contributed mostly by the conductance of the horizontal intracortical excitatory axons (Shlosberg et al., 2008), and not by polysynaptic connections as synchronized population waves of activity propagate (**Figure 4D**, Golomb and Amitai, 1997). In DAF-treated slices, LFPs at 1000 μm reached around 20% of their maximal amplitude. Furthermore, the horizontal decay pattern differed from control slices mainly due to a significant increase in the LFPs' relative amplitude at distances of 300–400 μm (**Figure 6C**), indicating that this region was particularly disinhibited. We then asked whether this finding was specific to the loss of NOS+ interneurons, or was a general feature of cortical disinhibition. We bathed the slices in low concentrations of PTX which

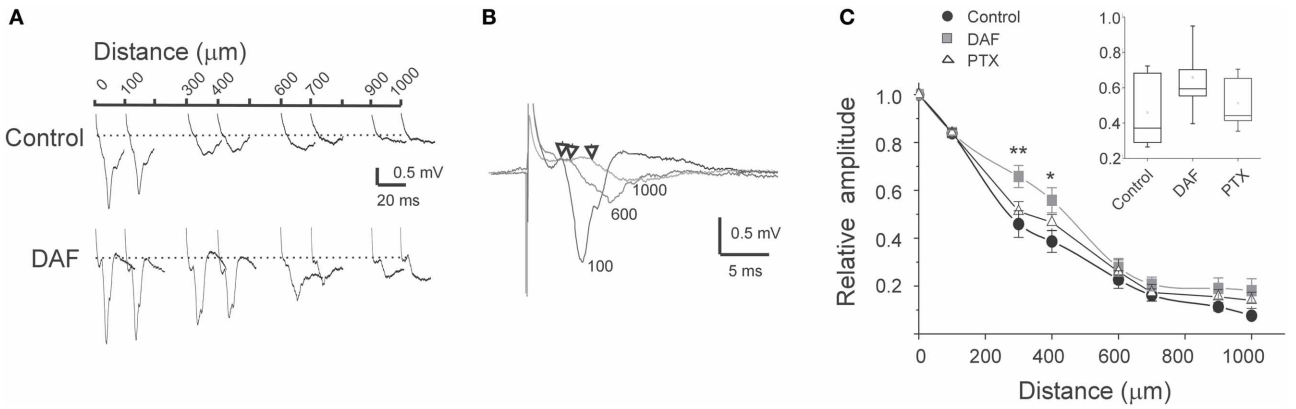

FIGURE 6 | The horizontal pattern of activity spread is affected by damage to NOS+ interneurons. (A) Example traces of simultaneously recorded LFPs at the distances as marked above, in control slice and in DAF-treated slice. **(B)** Example traces from simultaneous recordings of LFPs at three distances from the center of activation (marked by the traces, in μm). Arrows mark the deflection point from baseline. Note the short delay of around 3 ms for a distance of 1000 μm. **(C)** A summary diagram of the LFPs amplitude with distance, normalized to the amplitude above the stimulating electrode (distance 0), for control slices ($n = 16$), DAF-treated slices ($n = 13$), and PTX-treated slices ($n = 10$). Note a significant difference between control and DAF-treated slices at the distances of 300 μm ($p = 0.008$), and 400 μm ($p = 0.02$). The inset displayed the data distribution for the 300 μm point.

resulted in a similar distance of activity spread, and were subthreshold for the induction of synchronized events (3–5 μM). This dose of PTX resulted in a slightly reduced decay of LFPs horizontally compared with control slices, but the relative enhancement of activity at a distance of 300–400 μm was not observed (**Figure 6C**).

Inhibitory interneurons exhibit highly variable short-term dynamics of their synaptic activation. For example, among NOS+ interneurons, the subset of SOM+ cells are activated by pyramidal cells via uniquely facilitating synapses, such that they are strongly recruited at higher frequencies (Beierlein et al., 2003; Markram et al., 2004; Tan et al., 2008). We, therefore, hypothesized that when a single type of interneuron such as NOS+/SOM+ cells is selectively damaged, repetitive stimulation will result in even stronger alteration of the lateral activity spread pattern. Following the same recording scheme as before, we now applied six consecutive stimuli at 40 Hz and compared the spatio-temporal characteristics of activity between control and DAF-treated slices. Under control conditions, LFP frequency-dependent depression was monotonically reduced with distance (**Figure 7A**) while this order was interrupted in DAF-treated slices (**Figure 7B**). We next plotted the voltage attenuation as the ratio between the 6th and the 1st LFP amplitudes in the stimulus train (V6/V1) against the distance along the horizontal axis of the slice. Whereas untreated slices exhibited a highly linear correlation between the voltage attenuation ratio and the horizontal distance, this correlation was completely disrupted in DAF-treated slices (**Figure 7C**). The degree of activity depression at a given location may be correlated with the amplitude of the first LFP in the train, as higher amplitudes reflect higher activity levels of the network, and thus may engage stronger inhibition locally. We thus plotted V6/V1 against the amplitude of the first LFP (V1) at each recording site. Indeed, in control slices, the ratio V6/V1 was linearly correlated with V1 (**Figure 7D**). However, this relationship was not maintained in DAF-treated slices, implying that network recruitment with distance has been altered by the manipulation.

DISCUSSION

In this study we selectively damaged a population of NO-producing interneurons in cortical slices. This manipulation resulted in: (1) elongation of the decay time-constant and reduced dendritic delay of compound PSPs evoked on pyramidal neurons, (2) disinhibition of the network which was especially pronounced at horizontal distances of 300–400 μm from the center of activation, and (3) alterations of the spatio-temporal activity dynamics during repetitive stimulation. Together, our findings demonstrate directly, for the first time, a specific role for NOS+ interneurons in communicating significant lateral inhibition, and shaping the horizontal spread of activity.

THE IDENTITY OF DAF-POSITIVE NEURONS

The morphological identity of DAF-positive neurons was not established directly in this study due to technical difficulties. The few neurons that fluoresced during recording (**Figures 3C,D**) most likely belong to the NOS type I subgroup given their relatively large soma size. Yet, in the lack of direct morphological identification we have to rely on other studies. In the neocortex, nNOS is expressed exclusively by GABAergic neurons, and among them in several specific subpopulations with different expression levels (Kubota et al., 2011). Unsupervised clustering of cortical interneurons based on molecular, morphological, and electrophysiological parameters reveals two major groups (Karagiannis et al., 2009): the first one is relatively homogenous and consists of the FS, PV-expressing interneurons which do not expresses nNOS. Our finding which showed that FS neurons did not exhibit DAF-2DA fluorescence and maintained stable passive membrane properties under illumination is in agreement with these data. The second major cluster according to Karagiannis et al. (2009) exhibits considerable molecular diversity. Among neurons of

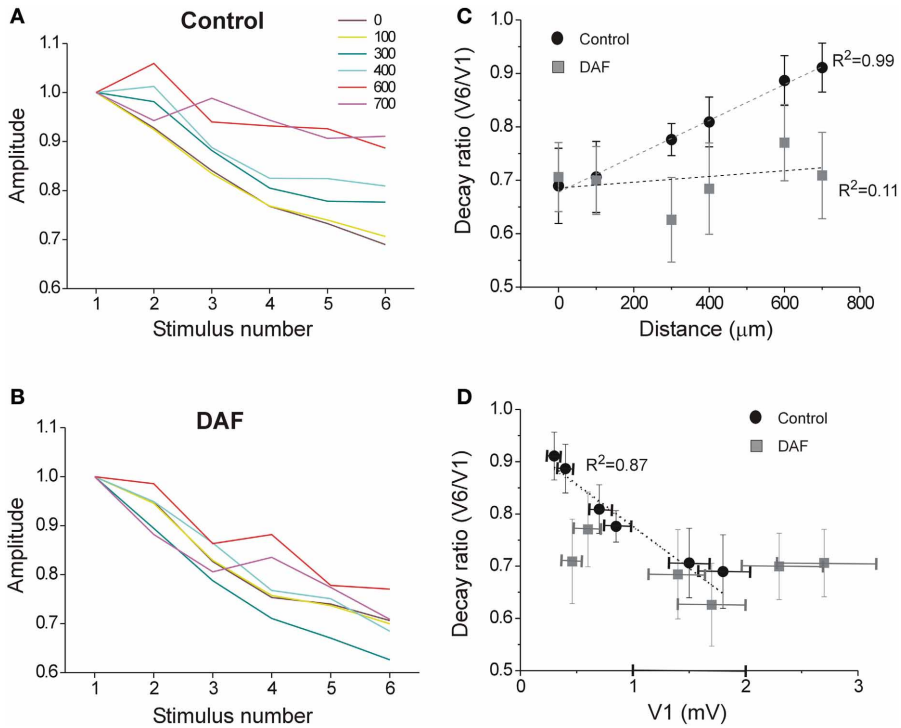

FIGURE 7 | The spatio-temporal dynamics of the network activity are disrupted in DAF-treated slices. A train of six stimuli at 40 Hz was delivered under the first electrode, and LFPs were recorded in layer 2/3 at six horizontal distances (color-coded as marked). **(A)** LFP depression with frequency is displayed for the six distance points in control slices. Each line displays an average of 10 slices (error bars omitted for clarity). **(B)** LFP depression with frequency is displayed for six distance points in DAF-treated slices. Each line displays an average of 11 slices. **(C)** For the same slices as in **A** and **B**, the ratio between the 6th and the 1st LFPs' amplitude is plotted as a function of the distance for control (black circles) and DAF-treated (gray squares) slices. Linear regression lines are plotted for each data set, and the adjusted *R*-square value is marked to the side. **(D)** The same ratio as in **(C)** is plotted as a function of the average amplitude of 1st LFP in the train, Linear regression line is plotted for the control data set. Data points in **(C)** and **(D)** display averages ± SEM.

this second non-fast-spiking cluster, nNOS was co-localized with some of the SOM− and NPY-expressing neurons.

Morphologically, SOM+ neurons have been largely characterized by long axonal projections targeting distal dendrites as well as the pyramidal apical tuft. A study examining synaptic target patterns of unidentified NOS+ neurons confirmed that they target dendritic segments of principal excitatory neurons (Seress et al., 2005). Another morphologically distinct subtype of NOS+ neurons has been associated with "neurogliaform" neurons. The extensive network of axons as revealed by the NADPH-d staining is indeed quite reminiscent of the axonal network of neurogliaform neurons. Interestingly, this type of interneurons is thought to deliver non-synaptic volume inhibition, devoid of any spatial selectivity (Oláh et al., 2009). Hence, we suggest that the more specific spatial alterations in the network behavior following damage to NOS+ interneurons, i.e., reduction of lateral inhibition, is mainly due to damage to the SOM+, dendritic targeting interneurons. NOS+ neurons indeed comprise a prevailing portion of interneurons with long axonal projections. The literature is very consistent and compelling in showing that NOS is expressed by a clear subset of SOM+ interneurons with relatively long axons in all species examined (monkey—Smiley et al., 2000; Tomioka and Rockland, 2007; cat—Higo et al., 2007; rat—Gonchar and Burkhalter, 1997; Vruwink et al., 2001).

Although NADPH-d staining was greatly diminished in treated slices, we cannot rule out that some NOS+ neurons remained. One of the reasons would be incomplete penetrance of the light to the depth of the 350 μm thick slices. DAF fluorescence was visible in the superficial 80–100 μm of the slices. Therefore, the physiological changes we documented are likely to reflect damage inflicted to some fraction of NOS+/SOM+ neurons. Interestingly, in several models of epilepsy, a selective loss of inhibitory SOM+ interneurons has been demonstrated (Sloviter, 1987; Robbins et al., 1991; Cossart et al., 2001). We speculate that the ability to produce NO renders these interneurons more vulnerable under conditions of high metabolic demands (Almeida et al., 2001), thus exacerbating the propensity to develop seizures.

CELLULAR EFFECTS OF NOS+ INTERNEURONS

NOS+/SOM+ interneurons are expected to target the distal dendritic branches. While several powerful mechanisms combine to amplify distal excitatory inputs, there are only a few recognized mechanisms that can support dendritic propagation of IPSPs (e.g., Williams and Stuart, 2003). Therefore, most theories regarding the role of distal dendritic inhibition maintain that it affects dendritic processing locally. By recording compound synaptic events on pyramidal neurons we unraveled several means by

which NOS+ interneurons might be affecting the summed activity. The increase in the EPSPs time constant can evolve directly from the removal of slow IPSPs, or from a secondary decrease in the activation of the hyperpolarization-activated cation channels (Ih), which are abundant in the distal dendrites of pyramidal cells (Gulledge et al., 2005). In both cases, the effect is elongation of the integration time window of neurons, allowing for stronger excitatory summation. Another interesting finding is the shortening of the dendritic delay. Cable theory suggests that the dendritic conduction velocity at a given point is equal to the ratio between the space constant and the time constant (Agmon-Snir and Segev, 1993). Given the increase in the time constant alone one would predict a reduction in the dendritic conduction velocity. On the other hand, the removal of dendritic inhibition is likely to enhance active conductances in the distal segments (Larkum et al., 1999; London and Hausser, 2005), thus enhancing the velocity of distal PSP's in their propagation toward the soma. Taken together these data imply that the damage inflicted to NOS+ neurons alters the overall integration properties of pyramidal neurons.

SPATIOTEMPORAL EFFECT OF NOS+ INTERNEURONS

Studies of cortical network activity have paid little attention to the horizontal, non-epileptic, spread of activity. It has been demonstrated that GABAergic inhibition controls the horizontal (tangential) spread of activity via intracortical connections (Chagnac-Amitai and Connors, 1989), but little is known about specific roles of interneurons subtypes in the spatial shaping of network activity. The short delay between the LFPs recorded at the column of stimulation and 1 mm away (around 3 ms) indicates that activity spread is mediated mostly by intracortical horizontal axons (Shlosberg et al., 2008). Such axons are well-documented, and indeed, monosynaptic horizontal EPSPs can be recorded in cortical slices up to distances of 1–3 mm (e.g., Hirsch and Gilbert, 1991; Telfeian and Connors, 2003). In our experimental setup, some detectable LFP remained 1 mm lateral to the stimulated column in control slices, and at slightly longer distances in disinhibited slices. However, the main difference between DAF-treated slices and controls appeared at horizontal distances of 300–400 μm. The size of a barrel column in the mouse somatosensory cortex is around 200 μm. Previous studies reveal specific interneurons in the barrel cortex with long horizontal axonal projections, expected to provide lateral inhibition (Kisvárday and Eysel, 1993; Helmstaedter et al., 2009). Our data strongly imply that NOS+ neurons provide such inhibition to neighboring columns. This role is in accordance with the anatomy of these neurons, which demonstrate that SOM+/NOS+ neurons have especially long axonal branches crossing columnar boundaries (e.g., Wang et al., 2004; Higo et al., 2007).

Excitatory transmission onto SOM+ interneurons is strongly facilitating, such that these interneurons are recruited by high activity rates (Beierlein et al., 2003; Markram et al., 2004; Silberberg and Markram, 2007; Tan et al., 2008). Given this information, we expected that selective damage to SOM+/NOS+ interneurons will result in reduced horizontal decay with repetitive stimulation, but the results do not support this simplistic hypothesis. We suggest that complex synaptic interactions between SOM+ interneurons and other neuronal types (Gibson et al., 1999) serve to compensate for their selective loss. Another surprising finding is the linear relationship between short-term depression of activity with repeated stimulation and the distance, or the local initial amplitude of the LFP, and the disruption of this relationship in DAF-treated slices. Frequency-dependent activity depression can be caused by the synaptic dynamics (both excitatory and inhibitory), and by the local recruitment of inhibitory neurons. The horizontal excitatory connection themselves demonstrate periodic variability in density (Chervin et al., 1988; Gilbert, 1993). Remarkably, all these parameters even-out in the control situation to yield a smooth reduction of frequency-dependent depression with distance and amplitude. We reason that once a subpopulation of interneurons is damaged, other cells in the network modify their activity rates, but the orderly architecture of network engagement is lost. Other means to selectively damage additional types of interneurons in the cortex will be needed to decipher their specific roles in controlling the spatial attributes of activity.

ACKNOWLEDGMENTS

The study was supported by grants 412/02 and 269/06 from the Israel Science Foundation to Yael Amitai. We thank D. Golomb for his useful comments on the manuscript.

REFERENCES

Agmon-Snir, H., and Segev, I. (1993). Signal delay and input synchronization in passive dendritic structures. *J. Neurophysiol.* 70, 2066–2085.

Almeida, A., Almeida, J., Bolanos, J. P., and Moncada, S. (2001). Different responses of astrocytes and neurons to nitric oxide: the role of glycolytically generated ATP in astrocyte protection. *Proc. Natl. Acad. Sci. U.S.A.* 98, 15294–15299.

Beierlein, M., and Connors, B. W. (2002) Short-term dynamics of thalamocortical and intracortical synapses onto layer 6 neurons in neocortex. *J. Neurophysiol.* 88, 1924–1932.

Beierlein, M., Gibson, J., and Connors, B. W. (2003). Two dynamically distinct inhibitory networks in layer 4 of the neocortex. *J. Neurophysiol.* 90, 2987–3000.

Buskila, Y., Farkash, S., Hershfinkel, M., and Amitai, Y. (2005). Rapid and reactive nitric oxide production by astrocytes in mouse neocortical slices. *Glia* 52, 169–176.

Cardin, J. A. (2011) Dissecting local circuits *in vivo*: integrated optogenetic and electrophysiology approaches for exploring inhibitory regulation of cortical activity. *J. Physiol. Paris* PMID: 21958624.

Cauli, B., Audinat, E., Lambolez, B., Angulo, M. C., Ropert, N., Tsuzuki, K., Hestrin, S., and Rossier, J. (1997). Molecular and physiological diversity of cortical nonpyramidal cells. *J. Neurosci.* 17, 3894–3906.

Chagnac-Amitai, Y., and Connors, B. W. (1989). Horizontal spread of synchronized activity in neocortex and its control by GABA-mediated inhibition. *J. Neurophysiol.* 61, 747–758.

Chagnac-Amitai, Y., Luhmann, H. J., and Prince, D. A. (1990). Burst generating and regular spiking layer 5 pyramidal neurons of rat neocortex have different morphological features. *J. Comp. Neurol.* 296, 598–613.

Chervin, R. D., Pierce, P. A., and Connors, B. W. (1988). Periodicity and directionality in the propagation of epileptiform discharges across neocortex. *J. Neurophysiol.* 60, 1695–1713.

Cossart, R., Dinoncourt, C., Hirsch, J. C., Merchan-Perez, A., De Felipe, J., Ben-Ari, Y., Esclapez, M., and Bernard, C. (2001). Dendritic but not somatic GABAergic inhibition is decreased in experimental epilepsy. *Nat. Neurosci.* 4, 52–62.

Felaco, M., Grilli, A., De Lutiis, M. A., Patruno, A., Libertini, N., Taccardi, A. A., Di Napoli, P., Di Giulio, C., Barbacane, R., and Conti, P. (2001). Endothelial nitric oxide synthase (eNOS) expression and localization in healthy and diabetic rat hearts. *Ann. Lab. Clin. Sci.* 31, 179–186.

Gibson, J. R., Beierlein, M., Connors, B. W. (1999) Two networks of electrically coupled inhibitory neurons in neocortex. *Nature* 402, 75–79.

Gilbert, C. D. (1993). Circuitry, architecture, and functional dynamics of visual cortex. *Cereb. Cortex* 3, 373–386.

Golomb, D., and Amitai, Y. (1997). Propagating neuronal discharges in neocortical slices: computational and experimental study. *J. Neurophysiol.* 78, 1199–1211.

Golomb, D., Donner, K., Shacham, L., Shlosberg, D., Amitai, Y., and Hansel, D. (2007). Mechanisms of firing patterns in fast-spiking cortical interneurons. *PLoS Comput. Biol.* 3, e156. doi: 10.1371/journal.pcbi.0030156

Golomb, D., and Ermentrout, B. G. (2001). Bistability in pulse propagation in networks of excitatory and inhibitory populations. *Phys. Rev. Lett.* 86, 4179–4182.

Gonchar, Y., and Burkhalter, A. (1997). Three distinct families of GABAergic neurons in rat visual cortex. *Cereb. Cortex* 7, 347–358.

Gulledge, A. T., Kampa, B. M., and Stuart, G. J. (2005). Synaptic integration in dendritic trees. *J. Neurobiol.* 64, 75–90.

Helmstaedter, M., Sakmann, B., and Feldmeyer, D. (2009). Neuronal correlates of local, lateral, and translaminar inhibition with reference to cortical columns. *Cereb. Cortex* 19, 926–937.

Higo, S., Udaka, N., and Tamamaki, N. (2007). Long-range GABAergic projection neurons in the cat neocortex. *J. Comp. Neurol.* 503, 421–431.

Hirsch, J. A., and Gilbert, C. D. (1991). Synaptic physiology of horizontal connections in the cat's visual cortex. *J. Neurosci.* 11, 1800–1809.

Hope, B. T., Michael, G. J., Knigge, K. M., and Vincent, S. R. (1991). Neuronal NADPH diaphorase is a nitric oxide synthase. *Proc. Natl. Acad. Sci. U.S.A.* 88, 2811–2814.

Kiss, J., Buzsáki, G., Morrow, J. S., Glantz, S. B., and Leranth, C. (1996). Entorhinal cortical innervation of parvalbumin-containing neurons (Basket and Chandelier cells) in the rat Ammon's horn. *Hippocampus* 6, 239–246.

Kapfer, C., Glickfeld, L. L., Attalah, B. V., and Scanziani, M. (2007). Supralinear increase of recurrent inhibition during sparse activity in the somatosensory cortex. *Nat. Neurosci.* 10, 743–753.

Karagiannis, A., Gallopin, T., Dávid, C., Battaglia, D., Geoffroy, H., Rossier, J., Hillman, E. M., Staiger, J. F., and Cauli, B. (2009). Classification of NPY-expressing neocortical interneurons. *J. Neurosci.* 29, 3642–3659.

Kawaguchi, Y. (1993). Grouping of nonpyramidal and pyramidal cells with specific physiological and morphological characteristics in rat frontal cortex. *J. Neurophysiol.* 69, 416–431.

Kawaguchi, Y., and Kubota, Y. (1993). Correlation of physiological subgroupings of nonpyramidal cells with Parvalbumin and Calbindin D28k-immunoreactive neurons in layer V of rat frontal cortex. *J. Neurophysiol.* 70, 387–396.

Kisvárday, Z. F., and Eysel, U. T. (1993). Functional and structural topography of horizontal inhibitory connections in cat visual cortex. *Eur. J. Neurosci.* 5, 1558–1572.

Kojima, H., Nakatsubo, N., Kikuchi, K., Kawahara, S., Kirino, Y., Nagoshi, H., Hirata, Y., and Nagano, T. (1998). Detection and imaging if nitric oxide with novel fluorescent indicators: diaminofluoresceins. *Anal. Chem.* 70, 2446–2453.

Kubota, Y., Shigematsu, N., Karube, F., Sekigawa, A., Kato, S., Yamaguchi, N., Hirai, Y., Morishima, M., and Kawaguchi, Y. (2011). Selective coexpression of multiple chemical markers defines discrete populations of neocortical GABAergic neurons. *Cereb. Cortex* 8, 1803–1817.

Larkum, M. E., Kaiser, K. M. M., and Sakmann, B. (1999). Calcium electrogenesis in distal apical dendrites of layer 5 pyramidal cells at a critical frequency of back-propagating action potentials. *Proc. Natl. Acad. Sci. U.S.A.* 96, 14600–14604.

Lee, J. E., and Jeon, C. J. (2005). Immunocytochemical localization of nitric oxide synthase-containing neurons in mouse and rabbit visual cortex and co-localization with calcium-binding proteins. *Mol. Cells* 19, 408–417.

London, M., and Hausser, M. (2005). Dendritic computation. *Annu. Rev. Neurosci.* 28, 503–532.

Lüth, H. J., Hedlich, A., Hilbig, H., Winkelmann, E., and Mayer, B. (1995). Postnatal development of NADPH-diaphorase/nitric oxide synthase positive nerve cells in the visual cortex of the rat. *J. Hirnforsch.* 36, 313–328.

Ma, Y., Hu, H., Berrebi, H. S., Mathers, P. H., and Agmon, A. (2006). Distinct subtypes of somatostatin-containing neocortical interneurons revealed in transgenic mice. *J. Neurosci.* 26, 5069–5082.

Markram, H., Toledo-Rodriguez, M., Wang, Y., Gupta, A., Silberberg, G., and Wu, C. (2004). Interneurons of the neocortical inhibitory system. *Nat. Neurosci. Rev.* 5, 793–806.

Oláh, S., Füle, M., Komlósi, G., Varga, C., Báldi, R., Barzó, P., and Tamás, G. (2009). Regulation of cortical microcircuits by unitary GABA-mediated volume transmission. *Nature* 461, 1278–1281.

Pouille, F., and Scanziani, M. (2002). Enforcement of temporal fidelity in pyramidal cells by somatic feed-forward inhibition. *Science* 293, 1159–1163.

Robbins, R. J., Brines, M. L., Kim, J. H., Adrian, T., de Lanerolle, N., Welsh, S., and Spencer, D. D. (1991). A selective loss of somatostatin in the hippocampus of patients with temporal lobe epilepsy. *Ann. Neurol.* 29, 325–332.

Salin, P. A., and Prince, D. A. (1996). Electrophysiological mapping of $GABA_A$ receptor-mediated inhibition in adult rat somatosensory cortex. *J. Neurophysiol.* 75, 1589–1600.

Seress, L., Abraham, H., Hajnal, A., Lin, H., and Totterdell, S. (2005). NOS-positive local circuit neurons are exclusively axo-dendritic cells both in the neo- and archi-cortex of the rat brain. *Brain Res.* 1056, 183–190.

Shlosberg, D., Abu-Ghanem, Y., and Amitai, Y. (2008). Comparative properties of excitatory and inhibitory inter-laminar neocortical axons. *Neuroscience* 155, 366–373.

Shlosberg, D., Patrick, S. L., Buskila, Y., and Amitai, Y. (2003). Inhibitory effect of mouse neocortex layer I on the underlying cellular network. *Eur. J. Neurosci.* 18, 2751–2759.

Silberberg, G., and Markram, H. (2007). Disynaptic inhibition between neocortical pyramidal cells mediated by Martinotti cells. *Neuron* 53, 735–746.

Sloviter, R. S. (1987). Decreased hippocampal inhibition and a selective loss of interneurons in experimental epilepsy. *Science* 235, 73–76.

Smiley, J. F., McGinnis, J. P., and Javitt, D. C. (2000). Nitric oxide synthase interneurons in the monkey cerebral cortex are subsets of the somatostatin, neuropeptide Y, and calbindin cells. *Brain Res.* 863, 205–212.

Sohal, V. S., Zhang, F., Yizhar, O., and Deisseroth, K. (2009). Parvalbumin neurons and gamma rhythms enhance cortical circuit performance. *Nature* 459, 698–702.

Tamamaki, N., and Tomioka, R. (2010). Long-range GABAergic connections distributed throughout the neocortex and their possible function. *Front. Neurosci.* 4, 202. doi: 10.3389/fnins.2010.00202

Tan, Z., Hu, H., Huang, Z. J., and Agmon, A. (2008). Robust but delayed thalamocortical activation of dendritic-targeting inhibitory interneurons. *Proc. Nat. Acad. Sci. U.S.A.* 105, 2187–2192.

Telfeian, A. E., and Connors, B. W. (2003). Widely integrative properties of layer 5 pyramidal cells support a role for processing of extralaminar synaptic inputs in rat neocortex. *Neurosci. Lett.* 343, 121–124.

Tomioka, R., and Rockland, K. S. (2007). Long-distance corticocortical GABAergic neurons in the adult monkey white and gray matter. *J. Comp. Neurol.* 505, 526–538.

Trevelyan, A. J., Sussillo, D., and Yuste, R. (2007). Feedforward inhibition contributes to the control of epileptiform propagation speed. *J. Neurosci.* 27, 3383–3387.

Uematsu, M., Hirai, Y., Karube, F., Ebihara, S., Kato, M., Abe, K., Obata, K., Yoshida, S., Hirabayashi, M., Yanagawa, Y., and Kawaguchi, Y. (2008). Quantitative chemical composition of cortical GABAergic neurons revealed in transgenic Venus-expressing rats. *Cereb. Cortex* 18, 315–330.

Valtschanoff, J. G., Weinberg, R. J., Kharazia, V. N., Schmidt, H. H., Nakane, M., and Rustioni, A. (1993). Neurons in rat cerebral cortex that synthesize nitric oxide: NADPH diaphorase histochemistry, NOS immunocytochemistry, and colocalization with GABA. *Neurosci. Lett.* 157, 157–161.

Vincent, S. R., and Kimura, H. (1992). Histochemical mapping of nitric oxide synthase in the rat brain. *Neuroscience* 46, 755–784.

Vruwink, M., Schmidt, H. H., Weinberg, R. J., and Burette, A. (2001). Substance P and nitric oxide signaling in cerebral cortex: anatomical evidence for reciprocal signaling between two classes of interneurons. *J. Comp. Neurol.* 441, 288–301.

Wang, Y., Toledo-Rodriguez, M., Gupta, A., Wu, C., Silberberg, G., Luo, J., and Markram, H. (2004). Anatomical, physiological and molecular properties of Martinotti cells in the somatosensory cortex of the juvenile rat. *J. Physiol.* 561, 65–90.

Williams, S. R., and Stuart, G. (2003). Voltage- and site-depenedent control of the somatic impact of dendritic IPSPs. *J. Neurosci.* 23, 7358–7367.

Conflict of Interest Statement: The authors declare that the research was conducted in the absence of any commercial or financial relationships that could be construed as a potential conflict of interest.

Received: 15 December 2011; accepted: 23 January 2012; published online: 07 February 2012.

Citation: Shlosberg D, Buskila Y, Abu-Ghanem Y and Amitai Y (2012) Spatiotemporal alterations of cortical network activity by selective loss of NOS-expressing interneurons. Front. Neural Circuits ***6****:3. doi: 10.3389/fncir.2012.00003*